SUPPORTING INFORMATION

An integrated methodology for the assessment of environmental health implications during thermal decomposition of nano-enabled products

Georgios A. Sotiriou[1], Dilpreet Singh[1], Fang Zhang[1], Wendel Wohlleben[1,2], Marie-Cecile G. Chalbot[3], Ilias G. Kavouras[3], Philip Demokritou[1]*

[1]Center for Nanotechnology and Nanotoxicology, Department of Environmental Health, School of Public Health, Harvard University, 665 Huntington Ave., Boston, MA 02115, USA.

[2]BASF SE, Material Physics, 67056 Ludwigshafen, Germany.

[3]Department of Environmental and Occupational Health, College of Public Health, University of Arkansas for Medical Sciences, Little Rock, AR 72205, USA

Corresponding author: pdemokri@hsph.harvard.edu

Submitted to:

Environmental Science: Nano

25 February 2015

MATERIALS AND METHODS

INEXS components

The NEP (approximately 100 mg) was placed in the quartz crucible in the form of pellets (~10 mm^3). Tube furnace #1 was acquired by Across International (model STF1200.60, 1200 ˚C Split Tube Furnace, 60 OD x 1000 mm Length) and tube furnace #2 by Carbolite Inc. (model GHA 12/900, 106.6 mm OD x 60" long 60 OD x 1524 mm Length). The gas analyzer (PCA 3 Model 285, Bacharach, Inc.) was positioned immediately after furnace #1. The thermal denuder was purchased by Dekati. All tubing in the system (conductive silicone rubber or stainless steel) and tube fittings were obtained by McMaster-Carr. The released aerosol was characterized *in situ* by SMPS or an APS, both TSI Inc.). Prior the analysis the aerosol was diluted using a rotating disk diluter or an aerosol diluter, respectively (TSI Inc.). The tVOC monitor (photo ionization based system, GrayWolf Sensing Solutions) was also placed after the disk diluter. The Harvard CCI[1] operates with three stages for the following size fractions: $PM_{2.5-10}$, $PM_{0.1-2.5}$ and $PM_{0.1}$. The PUF impaction substrates and Teflon/quartz filters (used to collect the $PM_{0.1}$ size fraction) from the CCI were weighed pre- and post-sampling following a 48 h stabilization process in a temperature- and humidity-controlled environmental chamber utilizing a Mettler Toledo XPE analytical microbalance. All sampling media (Teflon/quartz filters and PUF substrates) were chemically pre-cleaned in the laboratory to minimize background contamination using previously described protocols.[2]

NEP preparation and characterization

Polyurethane (PU) was synthesized via a prepolymer process. Chemtura Prepolymer Adiprene LF 930 and Ethacure 300 as chain extender are mixed thoroughly to produce cast PU. The nanoparticles used are MWNTs NC 7000 by Nanocyl. Synthesis of PU-CNT nanocomposites were carried out in two-steps process as follows. First, CNTs were added to prepolymer heated at 80 ˚C and mechanically stirred for 15 min at high shear of 2000 tr/min. At the second stage, a calculated amount of curative was added to the prepolymer nanocomposite and mixed again for one minute. The final mixture is degassed for one additional minute and poured in open mold at 100 ˚C to crosslink in 30 min and postcure in 20 hours. The final CNT concentration is 0.09 wt%. The CNT dispersion in the PU matrix was evaluated by transmission electron microscopy (TEM) of thin slices of the nanocomposites obtained by cryomicrotome (-140 ˚C). Figure S1 shows two

TEM images of a 1 μm thin slice of the model NEP (PU-CNT) used here at both low (a) and high magnification (b). The CNTs are homogeneously dispersed in the PU matrix.

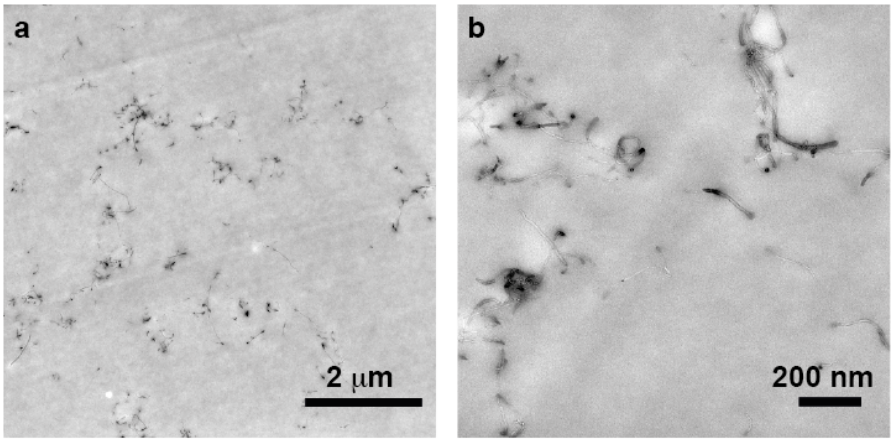

Figure S1. TEM images of the PU-CNT nanocomposite, revealing a number of dispersed CNTs in the PU matrix.

Physicochemical characterization of released aerosol and residual ash

The following different condition were examined as seen in Table S1 below.

Table S1. The different conditions used in this study.

Route	**$T_{d,final}$ (˚C)**	
I	500	800
II		800
III		800

Scanning electron microscopy (SEM) was performed on a Supra55VP Field Emission Scanning Electron Microscope. For the SEM sample preparation, collected size fractionated PM from PUF substrates and Teflon filters was extracted in pure EtOH by mild bath ultrasonication (30 s) and one drop from the resulting suspension was deposited in pre-cleaned Si wafer substrates and allowed to dry in ambient conditions.

Magnetic sector field inductively coupled plasma mass spectrometry (SF-ICPMS) was used for the evaluation of the elemental composition of the collected material (released aerosol and residual ash) following published protocols.[3] Briefly, the PM mass deposited on the PUF substrates, Teflon filters, and bulk powders was solubilized for total elemental analysis using a mixed acid (1.0 mL of 16M Nitric, 0.25 mL of 12M Hydrochloric, 0.1 mL of 28M Hydrofluoric) microwave-aided, digestion in sealed Teflon vials. The digest solutions were diluted to 15.0 mL with high-purity water (Millipore) in acid-washed low-density polyethylene (LDPE) bottles. Finally, the digested samples and extracts underwent SF-ICPMS

analysis (Thermo-Finnigan Element 2) for quantification of 50 elements. In addition to the collected samples, the analytical batches included sample spikes, sample duplicates, method and instrument blanks, and certified reference materials (NIST 2709, NIST 1648a, NIST 2556, NIST 2702) for quality assurance. Gas chromatography/mass spectrometry (GC/MS) was also performed to measure organic and elemental carbon levels.[4] The released aerosol was collected on pre-baked Quartz fiber filters. A one-cm^2 filter punch was used to measure OC-EC following the protocols standardized for the ACE-Asia intercomparison study.[4] This method is adapted from the NIOSH 5040 method, which utilizes Sunset Laboratory Inc. laboratory-based thermal optical analyzer.

One-dimensional proton nuclear magnetic resonance (1-D ^{1}H-NMR) spectroscopy was also applied to characterize the chemical content of organic carbon.[5,6] Each quartz filter was extracted sequentially with 5-ml of ethanol (C_2H_6O) for 1 hour in an ultrasonic bath to recover both the water- and organic-soluble species. Each extract was filtered on 0.45 μm polypropylene filter (Target2, Thermo Scientific), transferred into a pre-weighted vial (for the gravimetric determination of the total soluble extract, dried and re-dissolved in 250 μL of deuterated dimethylsulfoxide (DMSO; $(CD_3)_2SO$). A microbalance (Mettler-Toledo, Model: AB265-S) with precision of 10 μg was used in a temperature-controlled environment. DMSO is a universal polar solvent with superior to its ability to dissolve a wide range of water and organic-soluble species. The ^{1}H-NMR spectra were obtained on a Bruker Avance 500 MHz instrument equipped with a 5 mm double resonance broad band (BBFO Plus Smart) probe at 298K with 3,600 scans, using spin-lock, acquisition time of 3.2 s, relaxation delay of 1 s, and 1 Hz exponential line broadening and presaturation to the H_2O resonance.[5,6] Spectra were apodized by multiplication with an exponential decay corresponding to 1 Hz line broadening in the spectrum and a zero filling factor of 2. The baseline was manually corrected and integrated using the Advanced Chemistry Development NMR processor (Version 12.01 Academic Edition). The determination of chemical shifts (δ ^{1}H) was done relative to that of tetramethylsilate (TMS-d_{12}) (set at 0.0 ppm). The segment from δ 4.5 ppm to δ 5.0 ppm, corresponding to the water resonance, was removed from all NMR spectra. We applied the icoshift algorithm to align the NMR spectra[7] and integrated the intensity of signals of individual peaks as well as in five ranges.[8-11]

The saturated aliphatic region (*H*-C, δ 0.6 ppm – δ 1.8 ppm) was assumed to include protons from methyl, methylene and methine groups (R-C**H**$_3$, R-C**H**$_2$, and R-C**H**, respectively).[5,6,12] Aliphatic protons

bound to carbon adjacent to a double bond (**H**$_3$-C-C=) in the δ 1.8 - 3.1 ppm region were attributed to C-**H** adjacent to a carbonyl group (**H**-C-C=O), benzylic protons (Ar-C-**H**), allylic protons (**H**-C-C=C) and imino protons (**H**-C-C=N). Secondary or tertiary amines (**H**-C-NR$_2$) may also be present in the δ 2.2 ppm - δ 2.9 ppm region. The resonances in the δ 3.5 - 4.6 ppm region indicated the presence of hydroxyl functional group (-O**H**), and protons in carbons adjacent to hydroxy- (**H**-C-O) and ether-Hs (**H**-C-O-C) functional groups which are typically associated diols and polyhydroxy compounds. Vinylic-Hs (=C-**H**) (δ 4.6 - 6.5 ppm) region overlaps part of the region containing phenol (Ar-O**H**) signals in the δ 5.5 - 8.5 ppm region. Protons adjacent to C=N bonds (**H**-C=N) are typically found in the δ 8.5 - 10.9 ppm region, while carboxylic (-CO-O**H**) and phenolic-Hs (Ar-O**H**) are observed in the δ 10.9 - 12.3 ppm region.

RESULTS

Figures S2a,b show the O_2 and CO concentration during the TD as a function of time. The O_2 levels remain constant during the experiment and identical to ambient conditions ensuring O_2-rich conditions indicative of complete combustion. In contrast, there is a rapid CO evolution at similar time points as the maximum particle emission (Figure 2a,b) indicating the combustion process.

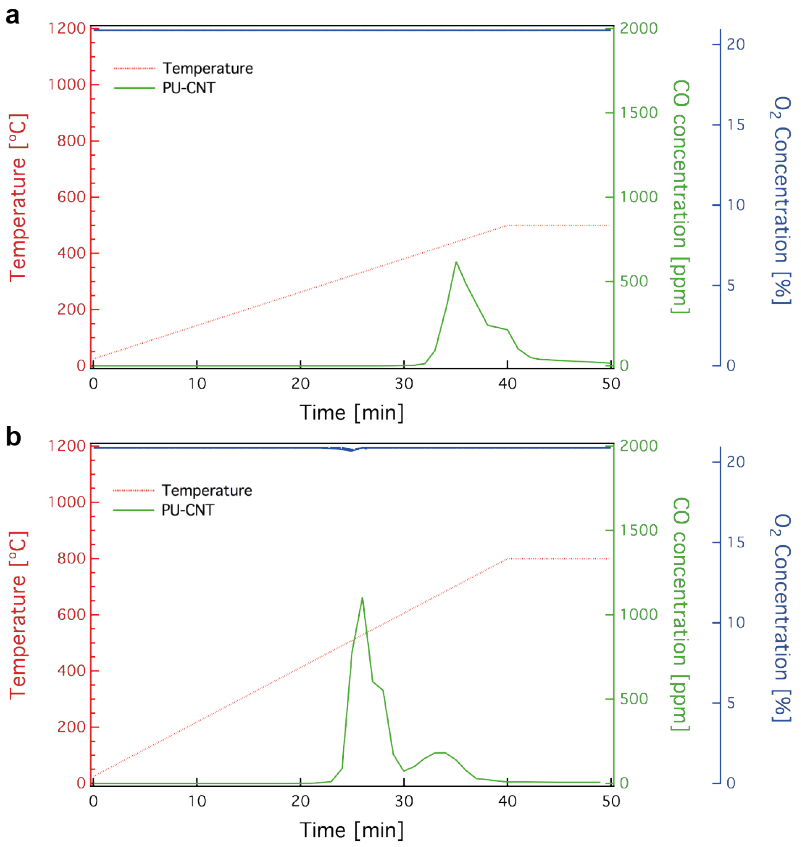

Figure S2. The CO and O_2 concentration levels are shown upon the TD of PU-CNT at $T_{d,final}$ = 500 (a) and 800 ˚C (b).

The mode mobility diameter from Figure 3a,b is also shown in Figure S3 for each $T_{d,final}$ = 500 (a) and 800 ˚C (b). The mode diameters also shift from low values reaching maximum at ~400 ˚C, and decreases at the end of combustion as a result of lower coagulation potential at lower particle concentrations.

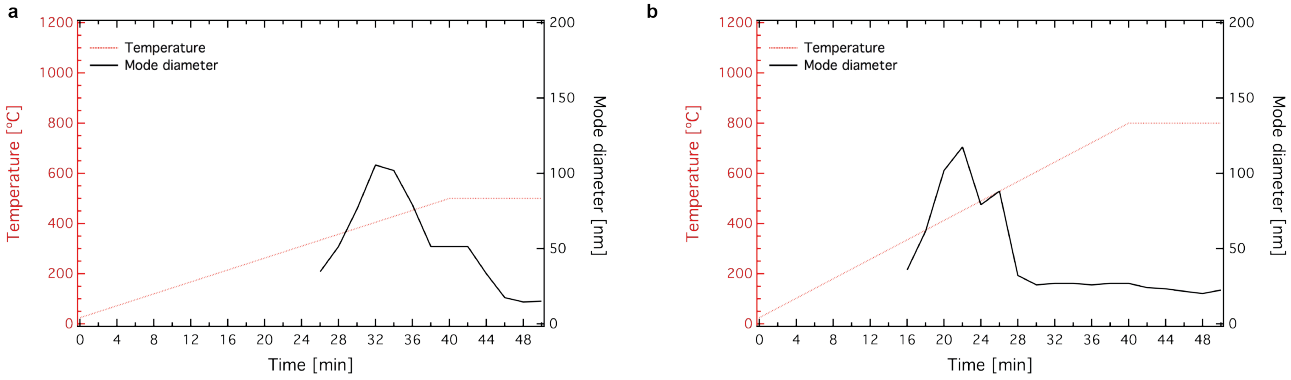

Figure S3. The SMPS mode mobility diameter as a function of time is presented for $T_{d,final}$ = 500 (a) and 800 ˚C (b).

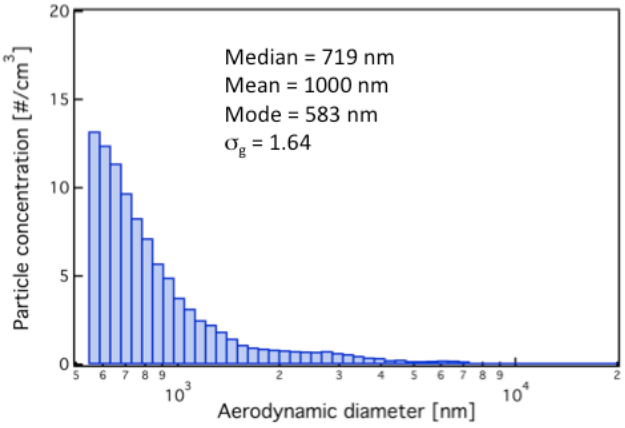

Figure S4. Aerodynamic particle size distribution for TD of PU-CNT at $T_{d,final}$ = 800 ˚C after 100 times dilution from route I.

Figure S5 shows the released aerosol particle mass distribution for $T_{d,final}$ = 500 (a) and 800 ˚C (b). Indeed, the largest PM size fraction by mass lies in the nano-regime (<100 nm), however, there are particles in the submicron- and micron-regime as well, in agreement with the real time data.

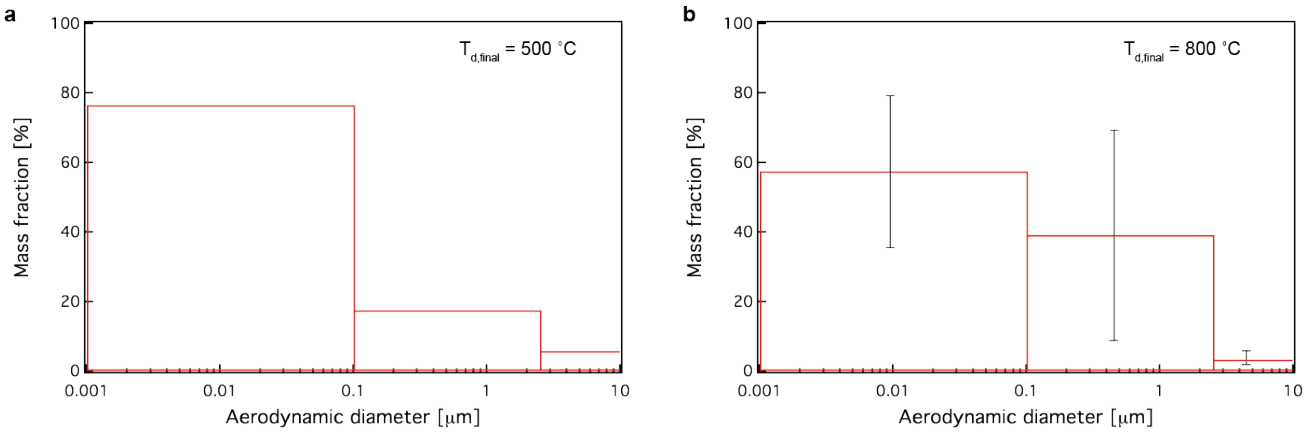

Figure S5. Particle size mass distributions for $T_{d,final}$ = 500 (a) and 800 °C (b) as obtained by gravimetric analysis of the CCI stages.

Thermal denuder losses

In order to evaluate the particle losses from the thermal denuder, the Harvard VENGES was utilized. We generated a model Ag aerosol following published protocols[13] and guided the generated SiO_2 aerosol through the thermal denuder at a flow rate of 5 L/min. Simultaneously, we measured the particle size and concentration (using SMPS) before and after the denuder. The tVOC content of the generated aerosol was ~600 ppb.

Figure S6a shows the average particle mobility size distribution of 3 individual experiments before (black line) and after the thermal denuder (red line) along with their standard deviation as error bars. From these distributions, the nanoparticle losses as a function of size can be calculated. Figure S6b shows the measured particle losses (%) as a function of mobility size (circles). Now, using these losses as a function of size, we can calculate the nominal losses from the thermal denuder for the released aerosol during a thermal decomposition experiment.

Figure S7 shows the particle concentration obtained from route I (solid line, before the denuder) and route II (broken line, after the denuder) as shown in Figure 3b and 8a, respectively. Figure S7 also shows the particle concentration as obtained assuming only particle losses (dotted line, per our calculations just above). It can be seen that the particle concentration derived from the denuder losses reaches much higher values than that of the actual measured from the thermal denuder. This indicates that there are indeed particle losses due to the thermal denuder, however, the measured reduced concentration is not only attributed to these losses, but mostly to the s/VOC removal.

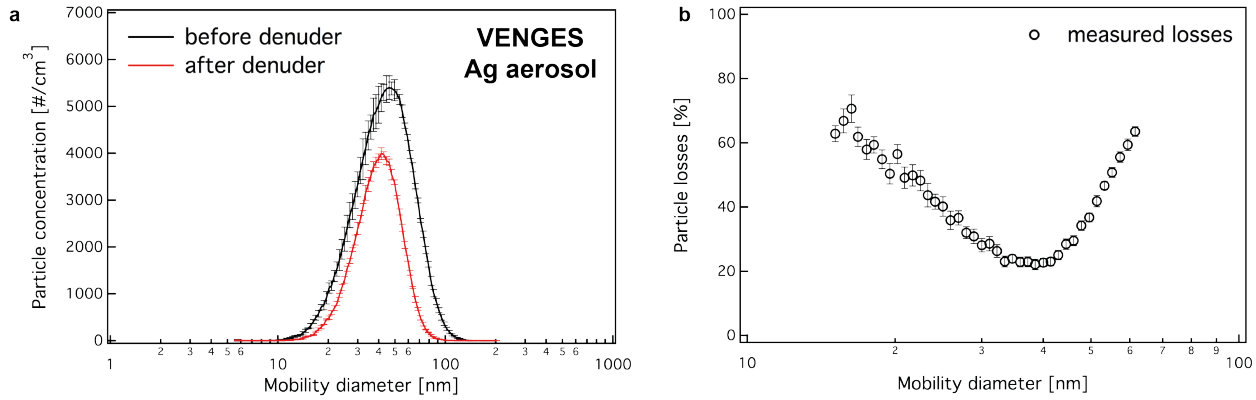

Figure S6. (a) The average particle mobility size distribution of 3 individual experiments before (solid line) and after the thermal denuder (broken red line) along with their standard deviation as error bars. (b) The measured particle losses (%) as a function of mobility size (circles).

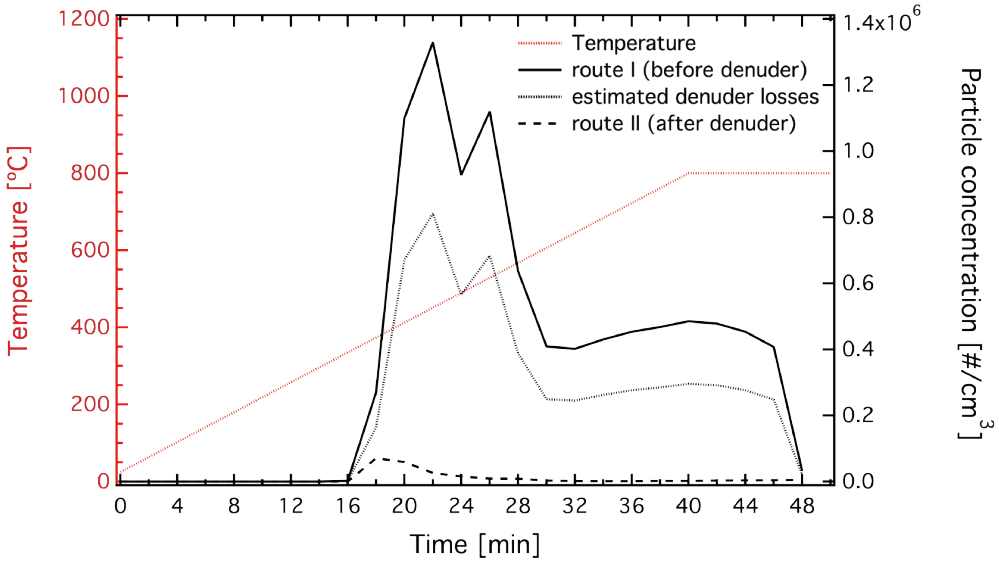

Figure S7. The mobility particle concentration upon the TD of PU-CNT at $T_{d,final}$ = 800 ˚C after 100 times dilution from route I (before thermal denuder, solid line), route II (after thermal denuder, broken line), and the estimated concentration from the denuder losses (dotted line).

NMR analysis

The ^{1}H-NMR spectra were characterized by a combination of sharp resonances of the most abundant organic species and convoluted resonances of many organic compounds present at low concentrations. The predominant resonances were those in the δ 1.25 ppm to δ 1.75 ppm range, followed by a set of resonances at the δ 0.80 - 0.95 ppm. They were previously attributed to terminal methyl groups, alkylic protons and protons bound on C=O in compounds with a combination of functional groups and long aliphatic

chains. These functional groups are typically present in isocyanate, urethane and urea, the primary products of polyurethane thermal decomposition (up to 350-400 °C) as well as their pyrolysis at higher temperatures.[14] In the δ 1.8-3.2 ppm range, a broad envelope of convoluted resonances were observed assigned primarily to imino, amino and benzylic protons, usually found in urea, an ingredient of polyurethane products. Two segments of resonances were observed in the δ 3.5 – 4.6 ppm region and attributed to hydrogen in α-position of an ester, ether, alcohol or acid groups (δ 4.1 to 4.25 ppm) and to hydrogen in α-position for an (N-C=O) bond, both of them present in polyurethane structures. The resonance at δ 5.75 ppm may be tentatively attributed to hydrogen atoms adjacent to a double bond in a cyclic structure.[15] The observed resonances were in agreement with previous studies on thermal decomposition of polyurethane through dissociation to isocyanate, alcohols, amine and olefins, and the formation of CO_2 and secondary amines in the 150-350 ˚C temperature range.[14-16] At higher temperatures, the formation of amines, cyclic oligomers as well as a strong polyol signature have previously been observed.[15,16]

During route I (without the denuder), the aliphatic fraction (δ 0.6 - 1.8 ppm) accounted for 42.7% of total non-exchangeable organic hydrogen concentration followed by the unsaturated region (δ 1.8 - 3.1 ppm) (26,1 %) and the aromatic (δ 6.5 - 8.5 ppm) region (13.7%). The δ 3.1 - 4.6 ppm and δ 4.6 - 6.5 ppm contributed 7.7 and 7.1%, respectively. For aerosol samples collected for the Route II configuration (with thermal denuder), the aliphatic-Hs were the dominant type accounting for 62.7% of total of non-exchangeable organic hydrogen concentration. The relative abundance of the unsaturated and aromatic ranges dropped to 17.5 and 9.6%, respectively. Similarly, the contribution of the two region in the carbohydrate region (δ 3.5 - 6.5 ppm) also declined to 5.4 and 3.0%, respectively.

The OC concentrations were 96.7 mmolC/m^3 and 36.3 mmolC/m^3 for Routes I and II, respectively, with a reduction of approximately 62.4% with the use of the thermal denuder (comparable to that computed for non-exchangeable organic hydrogen). The molar H/C ratio may provide information on the types of sources;[12] however, they should be cautiously evaluated because OC measurements may include OC that may not be soluble to ethanol, although previous studies showed that ethanol extraction efficiently was higher than 90%. H/C values higher than 2 were indicative of compounds with strong aliphatic components while H/C values from 1 to 2 were typically associated with oxygenated or nitro-organic species and H/C

values lower than 1 suggested an aromatic signature. The H/C molar ratios were 2.31 and 2.38 suggesting a strong aliphatic content.[6,12]

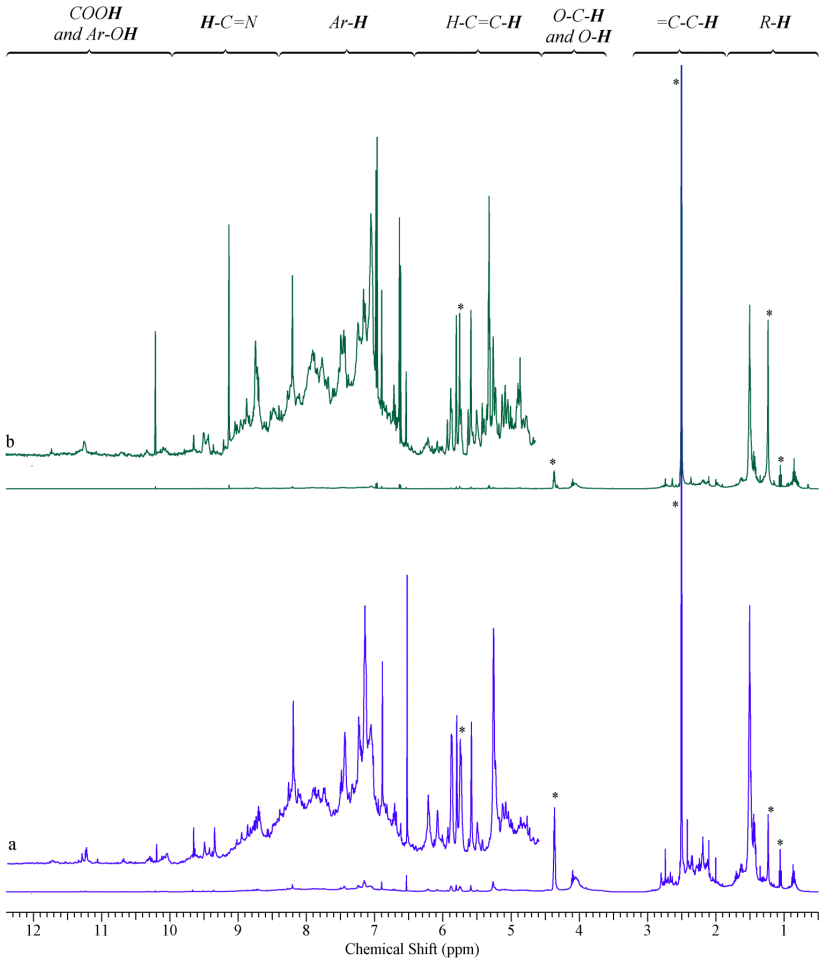

Figure S8. 500 MHz ^{1}H-NMR spectrum of the ethanol extract of the released aerosol during the TD of PU-CNT at at $T_{d,final}$ = 800 ˚C from route I (without the thermal denuder) (a) and route II (with the thermal denuder (b). The asterisk (*) indicates resonances associated with ethanol at δ 1.05 ppm, DMSO at δ 2.5 ppm and filter at δ 1.24 ppm and δ 5.75 ppm residues and excluded from the analysis.

References

1. Demokritou, P.; Lee, S. J.; Ferguson, S. T.; Koutrakis, P. A compact multistage (cascade) impactor for the characterization of atmospheric aerosols. *J. Aerosol. Sci.* **2004**, *35*, 281-299.
2. Bello, D.; Martin, J.; Santeufemio, C.; Sun, Q.; Lee Bunker, K.; Shafer, M.; Demokritou, P. Physicochemical and morphological characterisation of nanoparticles from photocopiers: implications for environmental health. *Nanotoxicology* **2012**, *7*, 989-1003.
3. Herner, J. D.; Green, P. G.; Kleeman, M. J. Measuring the trace elemental composition of size-resolved airborne particles. *Environ. Sci. Technol.* **2006**, *40*, 1925-33.

4. Schauer, J. J.; Mader, B. T.; Deminter, J. T.; Heidemann, G.; Bae, M. S.; Seinfeld, J. H.; Flagan, R. C.; Cary, R. A.; Smith, D.; Huebert, B. J.; Bertram, T.; Howell, S.; Kline, J. T.; Quinn, P.; Bates, T.; Turpin, B.; Lim, H. J.; Yu, J. Z.; Yang, H.; Keywood, M. D. ACE-Asia intercomparison of a thermal-optical method for the determination of particle-phase organic and elemental carbon. *Environ. Sci. Technol.* **2003**, *37*, 993-1001.
5. Chalbot, M.-C. G.; da Costa, G. G.; Kavouras, I. G. NMR analysis of the water-soluble fraction of airborne pollen particles. *Appl. Magn. Reson.* **2013**, *44*, 1347-1358.
6. Chalbot, M.-C. G.; Nikolich, G.; Etyemezian, V.; Dubois, D. W.; King, J.; Shafer, D.; da Costa, G. G.; Hinton, J. F.; Kavouras, I. G. Soil humic-like organic compounds in prescribed fire emissions using nuclear magnetic resonance spectroscopy. *Environ. Poll.* **2013**, *181*, 167-171.
7. Savorani, F.; Tomasi, G.; Engelsen, S. B. icoshift: A versatile tool for the rapid alignment of 1D NMR spectra. *J. Magn. Reson.* **2010**, *202*, 190-202.
8. Chalbot, M.-C. G.; Kavouras, I. G. Nuclear magnetic resonance spectroscopy for determining the functional content of organic aerosols: A review. *Environ. Poll.* **2014**, *191*, 232-249.
9. Decesari, S.; Facchini, M. C.; Fuzzi, S.; Tagliavini, E. Characterization of water-soluble organic compounds in atmospheric aerosol: A new approach. *J. Geophys. Res.-Atmos.* **2000**, *105*, 1481-1489.
10. Decesari, S.; Facchini, M. C.; Matta, E.; Lettini, F.; Mircea, M.; Fuzzi, S.; Tagliavini, E.; Putaud, J. P. Chemical features and seasonal variation of fine aerosol water-soluble organic compounds in the Po Valley, Italy. *Atmos. Environ.* **2001**, *35*, 3691-3699.
11. Suzuki, Y.; Kawakami, M.; Akasaka, K. H-1 NMR application for characterizing water-soluble organic compounds in urban atmospheric particles. *Environ. Sci. Technol.* **2001**, *35*, 2656-2664.
12. Chalbot, M.-C. G.; Brown, J.; Chitranshi, P.; da Costa, G. G.; Pollock, E. D.; Kavouras, I. G. Functional characterization of the water-soluble organic carbon of size-fractionated aerosol in the southern Mississippi Valley. *Atmos. Chem. Phys.* **2014**, *14*, 6075-6088.
13. Sotiriou, G. A.; Diaz, E.; Long, M. S.; Godleski, J.; Brain, J.; Pratsinis, S. E.; Demokritou, P. A novel platform for pulmonary and cardiovascular toxicological characterization of inhaled engineered nanomaterials. *Nanotoxicology* **2012**, *6*, 680-690.
14. Levchik, S. V.; Weil, E. D. Thermal decomposition, combustion and flame-retardancy of epoxy resins - a review of the recent literature. *Polymer Int.* **2004**, *53*, 1901-1929.
15. Lattimer, R. P.; Polce, M. J.; Wesdemiotis, C. MALDI-MS analysis of pyrolysis products from a segmented polyurethane. *J. Anal. Appl. Pyrol.* **1998**, *48*, 1-15.
16. Matuszak, M. L.; Frisch, K. C. Thermal-degradation of linear polyurethanes and model biscarbamates. *J. Polym. Sci. Pol. Chem.* **1973**, *11*, 637-648.